Miniature Ultra-Wideband Power Divider Using Bridged T-Coils

Yo-Shen Lin, *Senior Member, IEEE*, and Jun-Hua Lee

***Abstract*—In this work, a miniature ultra-wideband (UWB) power divider (PD) is proposed. By implementing the transmission lines of a two-stage Wilkinson PD using bridged T-coils, very compact size with no reduction in bandwidth can be achieved. Specifically, a proposed UWB two-way PD with a center frequency $f_0 = 5.5$ GHz is implemented using the commercial GaAs pHEMT process. The circuit size without pads is only 1.45 mm $\times$ 0.84 mm, which is about $0.027\lambda_0 \times 0.016\lambda_0$ at f_0. The fractional bandwidth for 15-dB input/output return loss and isolation is 110%, and the in-band insertion loss is within 1.3 $\pm$ 0.36 dB.**

***Index Terms*—Bridged T coil, GaAs, lumped-element, power divider (PD), ultra-wideband (UWB).**

I. Introduction

THE Wilkinson power divider (PD) is widely used in practical design due to its simple structure and good isolation between output ports. To achieve wider bandwidth, the multistage design [1] can be adopted. However, they occupy large circuit area due to the employment of multiple quarter-wavelength $(\lambda/4)$ lines. The size of Wilkinson PD can be largely reduced by using capacitive loadings [2] or lumped-element designs [3], [4]. However, the bandwidths of them are smaller compared to their transmission-line based counterparts. It is due to the fact that these equivalent transmission line structures match the response of the original transmission line at single frequency only. In order to obtain both wideband bandwidth and small circuit size, various ultra-wideband (UWB) PD structures have been proposed [5], [6]. In [6], by using the wafer-level packaging technique, a four-stage PD with a 2–22 GHz bandwidth has been achieved in a compact chip size of 4.75 mm $\times$ 3.20 mm.

In this work, a miniature UWB two-way PD is proposed, which can achieve more compact circuit size as compared to conventional UWB PD designs. It is realized by replacing the $\lambda/4$ lines in a two-stage Wilkinson PD using the bridged T-coil [7], [8]. In this way, the circuit size can be largely reduced but the bandwidth will remain about the same as compared with its transmission-line based counterpart.

Manuscript received March 14, 2012; revised June 05, 2012; accepted June 12, 2012. Date of publication July 05, 2012; date of current version August 03, 2012. This work was supported in part by the National Science Council of Taiwan under Grant NSC 99-2221-E-008-096-MY3 and Grant NSC 100-2628-E-008-010-MY3, and by the National Center for High-Performance Computing, Taiwan.

The authors are with the Department of Electrical Engineering, National Central University, Chungli 320, Taiwan (e-mail: yslin@ee.ncu.edu.tw).

Color versions of one or more of the figures in this letter are available online at http://ieeexplore.ieee.org.

Digital Object Identifier 10.1109/LMWC.2012.2205231

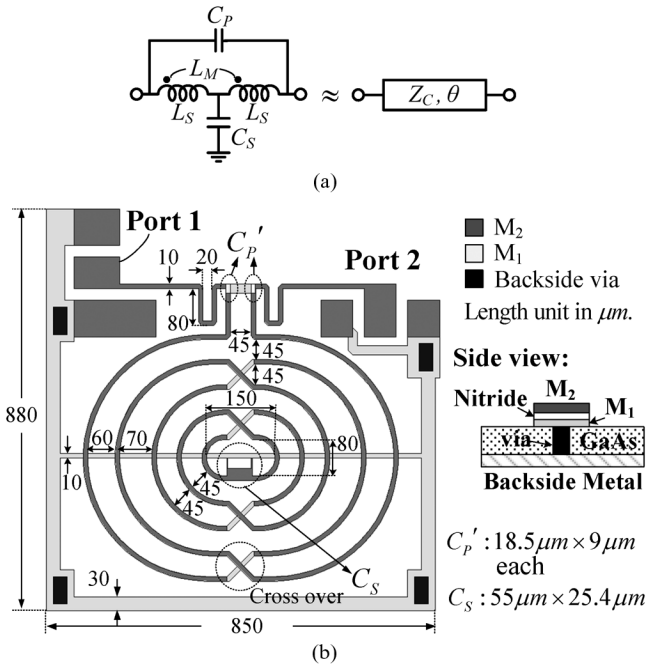

Fig. 1. (a) Bridged T-coil. (b) Layout of proposed lumped-element equivalent of transmission line in GaAs based on the bridged T-coil.

II. Circuit Design and Implementation

A. Lumped-Element Equivalent of Transmission Line

The bridged T-coil in Fig. 1(a) can achieve an all-pass response and thus is regarded as a constant-R network [8]. Therefore, it can be used as a wideband lumped-element equivalent of transmission line to realize microwave passive components in very compact sizes [9]. Given the required characteristic impedance $\mathrm{Z_C}$ and time delay, the required L and C values can be easily obtained using the equations in [10].

The bridged T-coil in Fig. 1(a) can be realized on chip in a very compact circuit size. Shown in Fig. 1(b) is the proposed circuit layout implemented using the WIN 0.5 $\mu\mathrm{m}$ E/D-mode pHEMT process on a 4-mil GaAs substrate [11]. The two metal layers $\mathrm{M_1}$ and $\mathrm{M_2}$ are gold with thickness of 1.1 and 2 $\mu\mathrm{m}$, respectively. Here the balanced spiral inductor structure along with a center tapped shunt metal-insulator-metal (MIM) capacitor formed by $\mathrm{M_1}, \mathrm{M_2}$, and the thin nitride layer in between are used to realize the two series inductors $\mathrm{L_S}$ and the shunt capacitor $\mathrm{C_S}$ in Fig. 1(a). The layout of the balanced inductor structure is properly designed such that the magnetic coupling between the two inductors of it $(\mathrm{L_S})$ can be equivalent to the required $\mathrm{L_M}$, while the electric coupling between them can be equivalent to the required $\mathrm{C_P}$. In case that the required $\mathrm{L_M}$ and $\mathrm{C_P}$ can not be achieved at the same time, the balanced inductor

is designed to achieve the required L_M first, and one additional series capacitor C'_P between the two ports can be introduced as shown in Fig. 1(b). Here, due to the required C'_p is quite small, two MIM capacitors in series are used. If the required L_M and C_P are already achieved but the corresponding L_S value of the balanced spiral inductor is not large enough, additional meander inductors at the input/output can be introduced as in Fig. 1(b).

The lumped circuit in Fig. 1(b) is designed to be equivalent to a $\lambda/4$ transmission line of $Z_C = 70.71\ \Omega$ at $f_0 = 2.45$ GHz. The required element values can be calculated as $L_S = 2.53$ nH, $C_S = 1.44$ pF, $L_M = 1.07$ nH, and $C_P = 0.15$ pF. The layout is first designed with the aid of a quasi-static solver Ansoft Q3D. Then, by using a full-wave simulator, e.g., Ansoft HFSS, one can extract the simulated two-port Z- and Y-parameters of the layout, and solve for the corresponding L and C values based on the equations of Z- and Y-parameters of the bridged T-coil available in [10] by neglecting the losses. Here, simulated Z- and Y-parameters at two frequencies around f_0 are selected to solve for the four distinct L and C values of the layout in closed-form. The layout is then properly adjusted until the target values of L and C are achieved with minimum errors.

Shown in Fig. 2 are the measured and simulated results. The measured return loss is better than 20 dB and the measured insertion loss is less than 1.25 dB from dc to 4.7 GHz. The measured ϕ_{21} is quite linear and is equal to 90° at 2.64 GHz. By using the method in [12], the measured $|Z_C|$ at 2.45 GHz is 73.9 Ω, and is within 70.71 ± 5% from 2.2 to 4 GHz. The imaginary part of Z_C is negative, which implies the power loss is mainly the conductor loss. Some deviations from the specified Z_C and electrical length are observed, which are due to the presence of other parasitic effects associated with the circuit layout. Anyway, the lumped circuit in Fig. 1(b) demonstrates very good similarity to a $\lambda/4$ transmission line in a wide frequency range as expected. Notably, its circuit size without pads is only $850\ \mu\text{m} \times 718\ \mu\text{m}$, which corresponds to $0.007\lambda_0 \times 0.006\lambda_0$ at 2.45 GHz. The measured β/k_o also achieves a high vale of 3.95 around 2.45 GHz, and the quality factor is 7.9.

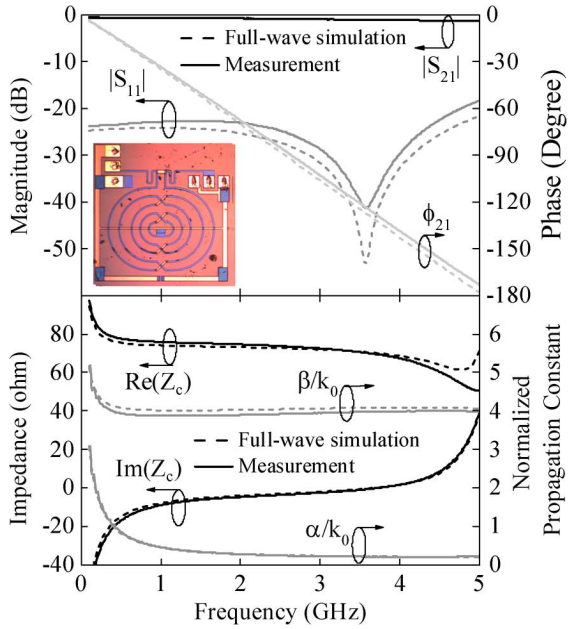

Fig. 2. Measured and full-wave simulated results of proposed lumped-element equivalent of transmission line (chip size: 1 mm × 1 mm). Reference impedances of the two-port S-matrix are set as 70.71 Ω.

B. Ultra-Wideband Two-Way Power Divider

The bridged T-coil can be used to implement an UWB PD in very compact size. Shown in Fig. 3(a) is a conventional two-stage Wilkinson PD, and its element values for a given specification can be obtained according to [1]. By replacing the $\lambda/4$ lines with the bridged T-coils [Fig. 3(b)], the circuit size can be largely reduced while the wideband characteristics can be maintained. Shown in Fig. 3(c) is a comparison between the frequency responses of the two PDs in Fig. 3 designed with an f_0 of 5.5 GHz. Here, the element values of the bridged T-coil are solved by equating its Z- and Y-parameters to those of the ideal transmission line at the two frequencies of 3.06 and 7.93 GHz when $|S_{11}| = 20$ dB, rather than using the formulae in [10] directly. In this way, a better match in frequency response can be achieved. As shown in Fig. 3(c), the frequency response of Fig. 3(b) is almost identical to that of its transmission-line based counterpart.

Based on the layout method in Fig. 1(b), the PD using bridged T-coils in Fig. 3(b) can also be implemented using the same GaAs pHEMT process. Shown in Fig. 4 is the circuit layout.

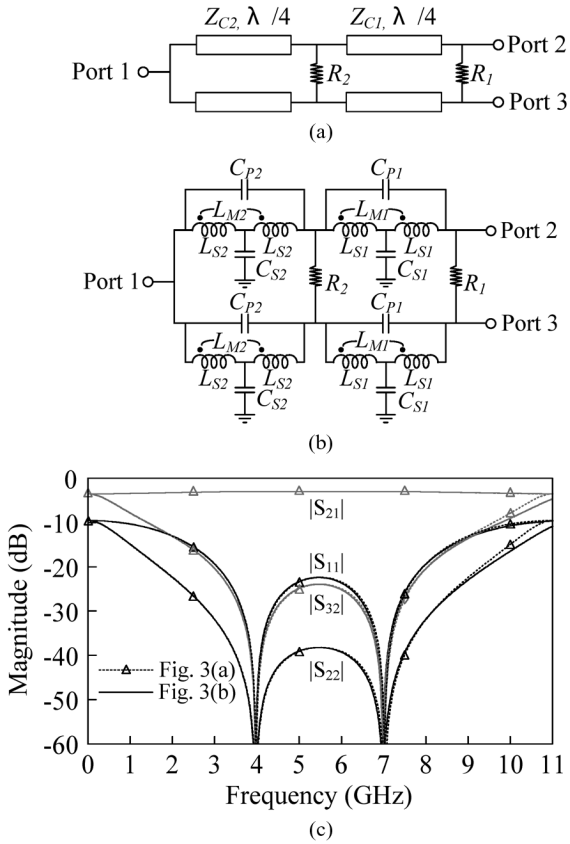

Fig. 3. (a) Conventional two-stage Wilkinson PD. ($Z_{c1} = 61.8\ \Omega$, $Z_{c2} = 81\ \Omega$, $R_1 = 226\ \Omega$, and $R_2 = 101.7\ \Omega$.) (b) Proposed UWB PD using bridged T-coils. ($L_{S1} = 0.958$ nH, $L_{M1} = 0.437$ nH, $C_{S1} = 0.731$ pF, $C_{P1} = 0.0683$ pF, $L_{S2} = 1.256$ nH, $L_{M2} = 0.573$ nH, $C_{S2} = 0.558$ pF, $C_{P2} = 0.0521$ pF, $R_1 = 226\ \Omega$, and $R_2 = 101.7\ \Omega$.) (c) Comparison in frequency response between these two PD designs.

The measured and simulated results are shown in Fig. 5. Although the frequency response of the GaAs PD deviates from that of the ideal circuit in Fig. 3(b) due to the power loss and

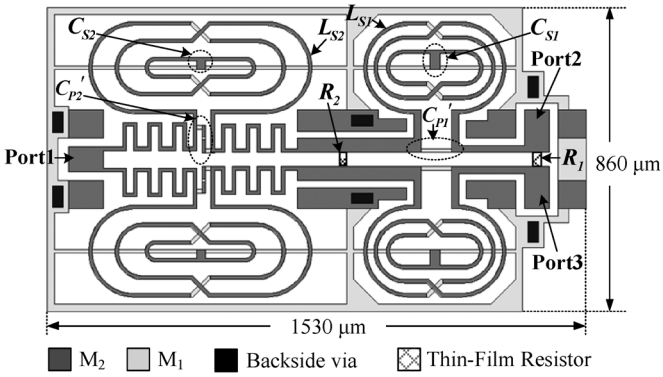

Fig. 4. Layout of proposed UWB PD in GaAs technology.

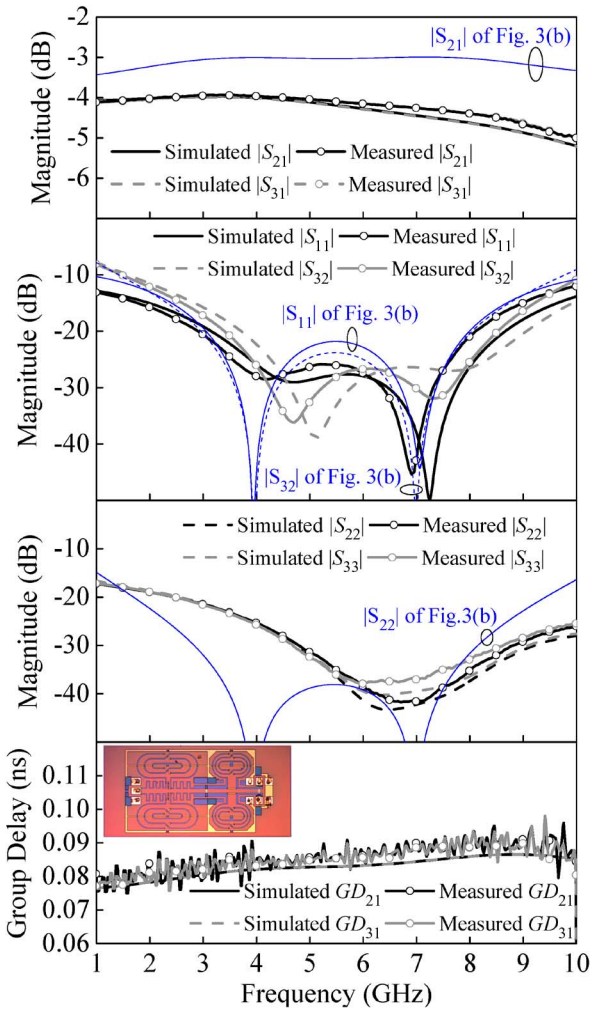

Fig. 5. Measured and simulated results of proposed UWB PD (chip size: 2 mm × 1 mm).

parasitic effects, very good performance is achieved. The measured input/output return losses and isolation are all better than 15 dB from 2.61 to 8.99 GHz, which corresponds to a bandwidth of 110%. The measured insertion losses are within 1.3 ± 0.36 dB and the group delays are within 0.086 ± 0.009 ns for the two signal paths in the same frequency range. Notably, the circuit size without pads is only 1.45 mm × 0.84 mm, which is about $0.027\lambda_0 \times 0.016\lambda_0$ at 5.5 GHz. The higher insertion loss is mainly caused by the thin conductor trace of the balanced inductor. The loss can be reduced by using wider conductor trace at the expense of larger circuit area.

III. Conclusion

An UWB two-way PD with very compact circuit size is proposed and implemented on chip. By using the bridged T-coil to replace the $\lambda/4$ transmission line in a conventional two-stage PD, the circuit size can be largely reduced with no reduction in bandwidth. It can also be applied to the design of higher stage PDs for even wider bandwidth, or be applied to the design of other transmission-line based microwave passive components to achieve good performance while reducing circuit size.

References

[1] S. B. Cohn, "A class of broadband three-port TEM-mode hybrids," *EEE Trans. Microw. Theory Tech.*, vol. MTT-19, no. 2, pp. 110–116, Feb. 1968.

[2] M. C. Scardelletti, G. E. Ponchak, and T. M. Weller, "Miniaturized Wilkinson power dividers utilizing capacitive loading," *IEEE Microw. Wireless Compon. Lett.*, vol. 12, no. 1, pp. 6–8, Jan. 2002.

[3] J.-G. Kim and G. M. Rebeiz, "Miniature four-way and two-way 24 GHz Wilkinson power dividers in 0.13 μm CMOS," *IEEE Microw. Wireless Compon. Lett.*, vol. 17, no. 9, pp. 658–660, Sep. 2007.

[4] M. M. Elsbury, P. D. Dresselhaus, N. F. Bergren, C. J. Burroughs, S. P. Benz, and Z. Popvic, "Broadband lumped-element integrated N-way power dividers for voltage standards," *IEEE Trans. Microw. Theory Tech.*, vol. 57, no. 8, pp. 2055–2063, Aug. 2009.

[5] S. W. Wong and L. Zhu, "Ultra-wideband power divider with good in-band splitting and isolation performances," *IEEE Microw. Wireless Comp. Lett.*, vol. 18, no. 8, pp. 518–520, Aug. 2008.

[6] X. Lan, P. Chang-Chien, F. Fong, D. Eaves, X. Zeng, and M. Kintis, "Ultra-wideband power divider using multi-wafer packaging technology," *IEEE Microw. Wireless Compon. Lett.*, vol. 21, no. 1, pp. 46–48, Jan. 2011.

[7] E. L. Ginzton, W. R. Hewlett, J. H. Jasberg, and J. D. Noe, "Distributed amplification," *Proc. IRE*, vol. 36, pp. 956–969, Aug. 1948.

[8] E. M. Chase and W. Kennan, "A power distributed amplifier using constant-R networks," in *IEEE MTT-S Int. Dig.*, Jun. 1986, pp. 811–815.

[9] Y.-S. Lin, C.-C. Liu, K.-M. Li, and C. H. Chen, "Design of an LTCC triband transceiver module for GPRS mobile applications," *IEEE Trans. Microw. Theory Tech.*, vol. 52, no. 12, pp. 2718–2723, Dec. 2004.

[10] T. S. Horng, J. M. Wu, L. Q. Yang, and S. T. Fang, "A novel modified-T equivalent circuit for modeling LTCC embedded inductors with a large bandwidth," in *IEEE MTT-S Int. Dig.*, Jun. 2003, pp. 1015–1018.

[11] WIN Semiconductor Corporation [Online]. Available: http://www.winfoundry.com/

[12] W. R. Eisenstadt and Y. Eo, "S-parameter-based IC interconnect transmission line characterization," *IEEE Trans. Comp., Hybrids, Manufact. Technol.*, vol. 15, no. 4, pp. 483–490, Aug. 1992.